Pulse compression of a high-power thin disk laser using rod-type fiber amplifiers

C. J. Saraceno,* O. H. Heckl, C. R. E. Baer, T. Südmeyer, and U. Keller

Department of Physics, Institute of Quantum Electronics, ETH Zurich, 8093 Zurich, Switzerland
**saraceno@phys.ethz.ch*

Abstract: We report on two pulse compressors for a high-power thin disk laser oscillator using rod-type fiber amplifiers. Both systems are seeded by a standard SESAM modelocked thin disk laser that delivers 16 W of average power at a repetition rate of 10.6 MHz with a pulse energy of 1.5 μJ and a pulse duration of 1 ps. We discuss two results with different fiber parameters and different trade-offs in pulse duration, average power, damage and complexity. The first amplifier setup consists of a Yb-doped fiber amplifier with a 2200 μm^2 core area and a length of 55 cm, resulting in a compressed average power of 55 W with 98-fs pulses at a repetition rate of 10.6 MHz. In the second system, a shorter 36-cm fiber with a larger core area of 4500 μm^2 is used. In a stretcher-free configuration we obtained 34 W of compressed average power and 65-fs pulses. In both cases peak powers of > 30 MW were demonstrated at several μJ pulse energies. The power scaling limitations due to damage and self-focusing are discussed.

OCIS codes: (140.0140) Lasers and laser optics; (320.7090) Ultrafast Lasers; (320.5520) Pulse Compression; (060.2320) Fiber optics amplifiers and oscillators.

References and links

1. U. Keller, D. A. B. Miller, G. D. Boyd, T. H. Chiu, J. F. Ferguson, and M. T. Asom, "Solid-state low-loss intracavity saturable absorber for Nd:YLF lasers: an antiresonant semiconductor Fabry-Perot saturable absorber," Opt. Lett. **17**(7), 505–507 (1992).
2. U. Keller, K. J. Weingarten, F. X. Kärtner, D. Kopf, B. Braun, I. D. Jung, R. Fluck, C. Hönninger, N. Matuschek, and J. Aus der Au, "Semiconductor saturable absorber mirrors (SESAMs) for femtosecond to nanosecond pulse generation in solid-state lasers," IEEE J. Sel. Top. Quantum Electron. **2**(3), 435–453 (1996).
3. U. Keller, "Recent developments in compact ultrafast lasers," Nature **424**(6950), 831–838 (2003).
4. U. Keller, "Ultrafast solid-state laser oscillators: a success story for the last 20 years with no end in sight," Appl. Phys. B **100**(1), 15–28 (2010).
5. T. Südmeyer, S. V. Marchese, S. Hashimoto, C. R. E. Baer, G. Gingras, B. Witzel, and U. Keller, "Femtosecond laser oscillators for high-field science," Nat. Photonics **2**(10), 599–604 (2008).
6. A. Giesen and J. Speiser, "Fifteen years of work on thin-disk lasers: results and scaling laws," IEEE J. Sel. Top. Quantum Electron. **13**(3), 598–609 (2007).
7. J. Aus der Au, G. J. Spühler, T. Südmeyer, R. Paschotta, R. Hövel, M. Moser, S. Erhard, M. Karszewski, A. Giesen, and U. Keller, "16.2-W average power from a diode-pumped femtosecond Yb:YAG thin disk laser," Opt. Lett. **25**(11), 859–861 (2000).
8. C. R. E. Baer, C. Kränkel, C. J. Saraceno, O. H. Heckl, M. Golling, R. Peters, K. Petermann, T. Südmeyer, G. Huber, and U. Keller, "Femtosecond thin-disk laser with 141 W of average power," Opt. Lett. **35**(13), 2302–2304 (2010).
9. T. Eidam, S. Hanf, E. Seise, T. V. Andersen, T. Gabler, C. Wirth, T. Schreiber, J. Limpert, and A. Tünnermann, "Femtosecond fiber CPA system emitting 830 W average output power," Opt. Lett. **35**(2), 94–96 (2010).
10. P. Russbueldt, T. Mans, J. Weitenberg, H. D. Hoffmann, and R. Poprawe, "Compact diode-pumped 1.1 kW Yb:YAG Innoslab femtosecond amplifier," Opt. Lett. **35**(24), 4169–4171 (2010).
11. J. Rothhardt, S. Hädrich, E. Seise, M. Krebs, F. Tavella, A. Willner, S. Düsterer, H. Schlarb, J. Feldhaus, J. Limpert, J. Rossbach, and A. Tünnermann, "High average and peak power few-cycle laser pulses delivered by fiber pumped OPCPA system," Opt. Express **18**(12), 12719–12726 (2010).
12. S. V. Marchese, C. R. E. Baer, A. G. Engqvist, S. Hashimoto, D. J. H. C. Maas, M. Golling, T. Südmeyer, and U. Keller, "Femtosecond thin disk laser oscillator with pulse energy beyond the 10-microjoule level," Opt. Express **16**(9), 6397–6407 (2008).
13. J. Neuhaus, D. Bauer, J. Zhang, A. Killi, J. Kleinbauer, M. Kumkar, S. Weiler, M. Guina, D. H. Sutter, and T. Dekorsy, "Subpicosecond thin-disk laser oscillator with pulse energies of up to 25.9 microjoules by use of an active multipass geometry," Opt. Express **16**(25), 20530–20539 (2008).

#138059 - $15.00 USD Received 15 Nov 2010; revised 16 Dec 2010; accepted 20 Dec 2010; published 12 Jan 2011

14. C. J. Saraceno, C. Schriber, M. Mangold, M. Hoffmann, O. H. Heckl, C. R. E. Baer, M. Golling, T. Sudmeyer, and U. Keller, "SESAMs for high-power oscillators: design guidelines and damage thresholds," IEEE J. Sel. Top. Quantum Electron. (to be published).
15. T. Südmeyer, C. Kränkel, C. R. E. Baer, O. H. Heckl, C. J. Saraceno, M. Golling, R. Peters, K. Petermann, G. Huber, and U. Keller, "High-power ultrafast thin disk laser oscillators and their potential for sub-100-femtosecond pulse generation," Appl. Phys. B **97**(2), 281–295 (2009).
16. F. Brunner, T. Südmeyer, E. Innerhofer, F. Morier-Genoud, R. Paschotta, V. E. Kisel, V. G. Shcherbitsky, N. V. Kuleshov, J. Gao, K. Contag, A. Giesen, and U. Keller, "240-fs pulses with 22-W average power from a mode-locked thin-disk Yb:KY$(WO_4)_2$ laser," Opt. Lett. **27**(13), 1162–1164 (2002).
17. O. H. Heckl, C. Kränkel, C. R. E. Baer, C. J. Saraceno, T. Südmeyer, K. Petermann, G. Huber, and U. Keller, "Continuous-wave and modelocked Yb:YCOB thin disk laser: first demonstration and future prospects," Opt. Express **18**(18), 19201–19208 (2010).
18. G. Palmer, M. Schultze, M. Siegel, M. Emons, U. Bünting, and U. Morgner, "Passively mode-locked Yb:KLu$(WO_4)_2$ thin-disk oscillator operated in the positive and negative dispersion regime," Opt. Lett. **33**(14), 1608–1610 (2008).
19. C. R. E. Baer, C. Kränkel, C. J. Saraceno, O. H. Heckl, M. Golling, T. Südmeyer, R. Peters, K. Petermann, G. Huber, and U. Keller, "Femtosecond Yb:Lu_2O_3 thin disk laser with 63 W of average power," Opt. Lett. **34**(18), 2823–2825 (2009).
20. C. R. E. Baer, C. Kränkel, O. H. Heckl, M. Golling, T. Südmeyer, R. Peters, K. Petermann, G. Huber, and U. Keller, "227-fs pulses from a mode-locked Yb:$LuScO_3$ thin disk laser," Opt. Express **17**(13), 10725–10730 (2009).
21. D. Grischkowsky and A. C. Balant, "Optical pulse compression based on enhanced frequency chirping," Appl. Phys. Lett. **41**(1), 1–3 (1982).
22. C. V. Shank, R. L. Fork, R. Yen, R. H. Stolen, and W. J. Tomlinson, "Compression of femtosecond optical pulses," Appl. Phys. Lett. **40**(9), 761–763 (1982).
23. T. Südmeyer, F. Brunner, E. Innerhofer, R. Paschotta, K. Furusawa, J. C. Baggett, T. M. Monro, D. J. Richardson, and U. Keller, "Nonlinear femtosecond pulse compression at high average power levels by use of a large-mode-area holey fiber," Opt. Lett. **28**(20), 1951–1953 (2003).
24. E. Innerhofer, F. Brunner, S. V. Marchese, R. Paschotta, U. Keller, K. Furusawa, J. C. Baggett, T. M. Monro, and D. J. Richardson, "32 W of average power in 24-fs pulses from a passively mode-locked thin disk laser with nonlinear fiber compression," in *Advanced Solid-State Photonics (ASSP)* (Optical Society of America, 2005), paper TuA3.
25. J. Limpert, O. Schmidt, J. Rothhardt, F. Röser, T. Schreiber, A. Tünnermann, S. Ermeneux, P. Yvernault, and F. Salin, "Extended single-mode photonic crystal fiber lasers," Opt. Express **14**(7), 2715–2720 (2006).
26. D. N. Papadopoulos, Y. Zaouter, M. Hanna, F. Druon, E. Mottay, E. Cormier, and P. Georges, "Generation of 63 fs 4.1 MW peak power pulses from a parabolic fiber amplifier operated beyond the gain bandwidth limit," Opt. Lett. **32**(17), 2520–2522 (2007).
27. Y. Zaouter, D. N. Papadopoulos, M. Hanna, J. Boullet, L. Huang, C. Aguergaray, F. Druon, E. Mottay, P. Georges, and E. Cormier, "Stretcher-free high energy nonlinear amplification of femtosecond pulses in rod-type fibers," Opt. Lett. **33**(2), 107–109 (2008).
28. S. V. Marchese, T. Südmeyer, M. Golling, R. Grange, and U. Keller, "Pulse energy scaling to 5 μJ from a femtosecond thin disk laser," Opt. Lett. **31**(18), 2728–2730 (2006).
29. M. Haiml, R. Grange, and U. Keller, "Optical characterization of semiconductor saturable absorbers," Appl. Phys. B **79**(3), 331–339 (2004).
30. D. J. H. C. Maas, B. Rudin, A.-R. Bellancourt, D. Iwaniuk, S. V. Marchese, T. Südmeyer, and U. Keller, "High precision optical characterization of semiconductor saturable absorber mirrors," Opt. Express **16**(10), 7571–7579 (2008).
31. E. B. Treacy, "Optical pulse compression with diffraction gratings," IEEE J. Quantum Electron. **5**(9), 454–458 (1969).
32. R. Trebino and D. J. Kane, "Using phase retrieval to measure the intensity and phase of ultrashort pulses: frequency-resolved optical gating," J. Opt. Soc. Am. A **10**(5), 1101–1111 (1993).
33. I. Martial, D. Papadopulos, M. Hanna, F. Druon, and P. Georges, "Nonlinear compression in a rod-type fiber for high energy ultrashort pulse generation," Opt. Express **17**(13), 11155–11160 (2009).
34. A. V. Smith, B. T. Do, G. R. Hadley, and R. L. Farrow, "Optical damage limits to pulse energy from fibers," IEEE J. Sel. Top. Quantum Electron. **15**(1), 153–158 (2009).
35. A. V. Smith and B. T. Do, "Bulk and surface laser damage of silica by picosecond and nanosecond pulses at 1064 nm," Appl. Opt. **47**(26), 4812–4832 (2008).
36. K. P. Hansen, NKT Photonics, private communication, (2010).
37. M. E. Fermann, V. I. Kruglov, B. C. Thomsen, J. M. Dudley, and J. D. Harvey, "Self-similar propagation and amplification of parabolic pulses in optical fibers," Phys. Rev. Lett. **84**(26), 6010–6013 (2000).
38. Y. Zaouter, D. N. Papadopoulos, M. Hanna, F. Druon, E. Cormier, and P. Georges, "Third-order spectral phase compensation in parabolic pulse compression," Opt. Express **15**(15), 9372–9377 (2007).
39. S. Hädrich, J. Rothhardt, T. Eidam, J. Limpert, and A. Tünnermann, "High energy ultrashort pulses via hollow fiber compression of a fiber chirped pulse amplification system," Opt. Express **17**(5), 3913–3922 (2009).
40. C. P. Hauri, W. Kornelis, F. W. Helbing, A. Heinrich, A. Couairon, A. Mysyrowicz, J. Biegert, and U. Keller, "Generation of intense, carrier-envelope phase-locked few-cycle laser pulses through filamentation," Appl. Phys. B **79**(6), 673–677 (2004).

#138059 - $15.00 USD Received 15 Nov 2010; revised 16 Dec 2010; accepted 20 Dec 2010; published 12 Jan 2011

1. Introduction

Modelocked thin disk lasers using a semiconductor saturable absorber mirror (SESAM) [1,2] for passive pulse formation are currently one of best-suited technologies for ultrafast high-power laser oscillators [3–5]. They benefit from excellent thermal handling and power scalability of both the thin disk laser head [6] and the SESAM. Indeed, since the first demonstration of a SESAM modelocked thin disk laser [7], this approach resulted in higher output powers than any other femtosecond oscillator. The current power record is 140 W in 738-fs pulses [8], and further power scaling to the kilowatt regime appears feasible. Other approaches for ultrafast laser systems at high average power levels are fiber-based chirped pulse amplification (CPA) [9] and Innoslab amplifiers [10], which can be temporally compressed using high power OPCPA schemes [11].

A key advantage of the thin disk laser compared to other concepts is the very low accumulated intracavity nonlinearity mostly introduced by the disk and the cavity optics, which are all used in reflection. Pulse energies as high as 11.3 μJ were generated in a one-pass cavity geometry using the thin disk as a simple folding mirror [12] and 25.9 μJ were achieved in an active multi-pass cavity with 13 reflections on the disk [13]. SESAMs are ideally suited for high-power modelocking because of their high damage thresholds [14]. The complexity of these multi-100-Watt lasers is not higher than that of low-power oscillators. They will therefore replace complex amplifier systems for many applications and their new performance parameters with higher megahertz pulse repetition rates and better noise properties will enable new applications.

Many experiments in areas such as high field science require pulse durations in the sub-100-fs regime, which has not been demonstrated with thin disk lasers so far. The first demonstrations of power and energy scaling of modelocked thin disk lasers were achieved with the well-established gain material Yb:YAG. The gain bandwidth limits in this case the achievable pulse duration in high-power operation to ≈700 fs. There are more than ten Yb-doped gain materials that have generated sub-100-fs pulses in standard low-power oscillators, and great efforts have been dedicated during the past few years to extend this performance into the high power regime [15]. Using Yb:KYW, 22W of average power were demonstrated in 240 fs pulses [16]. Other tested thin disk materials include Yb:YCOB (2 W, 270 fs [17],), Yb:KLuW (25 W, 440 fs [18]), and Yb:Lu_2O_3 (40 W, 329 fs [19]). The shortest pulses achieved so far are 227 fs from Yb:$LuScO_3$ [20]. However, in this case a poor disk quality limited the average power to 7.2 W. Reaching the sub-100-fs regime appears feasible but challenging. Therefore, other alternatives such as fiber pulse compression [21,22] represent a simple and interesting alternative.

Previously, pulse compression of a SESAM modelocked high-power thin disk laser has been demonstrated using a short passive LMA fiber where 32 W and 24 fs pulses were demonstrated at MHz repetition rate [23,24]. In this experiment, the initially 760-fs long pulses were compressed at 50% efficiency by a factor of thirty, while the peak power was increased by a factor of ten. This method enabled high field science experiments driven directly at the multi-megahertz repetition rate of the femtosecond oscillator [5]. This passive compression system suffered, however, from severe limitations. Damage in the 200-μm^2 mode-area fiber limited the maximum achievable compressed pulse energy to less than 1 μJ. It seems difficult to generate substantially higher pulse energies with standard microstructured LMA fibers with larger mode areas because the weak guiding results in high bending sensitivity and losses.

We therefore applied an interesting alternative to overcome these limitations using an active LMA rod-type fiber compressor that also provides amplification [25]. In this case, the bending sensitivity is reduced by surrounding the fiber with a glass rod, therefore allowing for stable single-mode operation with much larger mode sizes. Typically, commercially available rod-type fiber amplifiers have fundamental mode areas up to 4500 μm^2, which is larger than any other fiber technology. Furthermore, these fibers are well suited for polarization-maintaining operation even at high peak power levels using stress-induced birefringence.

#138059 - $15.00 USD Received 15 Nov 2010; revised 16 Dec 2010; accepted 20 Dec 2010; published 12 Jan 2011

Previously, pulse compression of low and medium power level oscillators using these rod-type fiber amplifiers has been demonstrated in different setups where MW peak powers at MHz repetition rates were achieved [26,27].

In this paper, we discuss pulse compression of a standard high-power SESAM modelocked Yb:YAG thin disk laser using LMA rod-type fiber amplifiers. The high seed power allows for one single main amplifier stage, which is directly saturated without the need for additional preamplifier stages. We present two compressor systems of a thin disk laser oscillator using two different rod-type fiber amplifiers. In the first system, we used a 55-cm long rod with a core area of 2200 μm^2, and achieved 55 W of compressed average power in 98-fs pulses, reaching pulse energy of 5.2 µJ at 10.6 MHz and a peak power of 32.7 MW. In a second system no pulse stretcher was required using a 36-cm rod-type fiber amplifier with a larger core area of 4500 μm^2. With this setup 34 W of average power were demonstrated in 65-fs pulses, reaching a similar peak power of 32 MW. We will discuss the performance and power scaling limitations of these two systems, in particular concerning damage and self-focusing.

2. Experimental setups and results

The seed laser used for both amplifier systems consists of a standard Yb:YAG SESAM modelocked thin disk laser similar to the one described in [28] that delivers 16 W of average output power at a repetition rate of 10.6 MHz at a central wavelength of 1030 nm. This corresponds to a pulse energy of 1.5 µJ in 1-ps-long pulses (Fig. 1). The corresponding intracavity energy of 12.8 µJ is low enough for stable operation in air. The SESAM used in this laser has a dielectric top-section for high damage threshold and low parasitic losses [14]. Using a home-build setup for nonlinear optical reflectivity characterization [29,30], we measured a saturation fluence F_{sat} = 46 µJ/cm^2, a modulation depth ΔR = 0.58% and nonsaturable losses $\Delta R_{ns} < 0.1\%$.

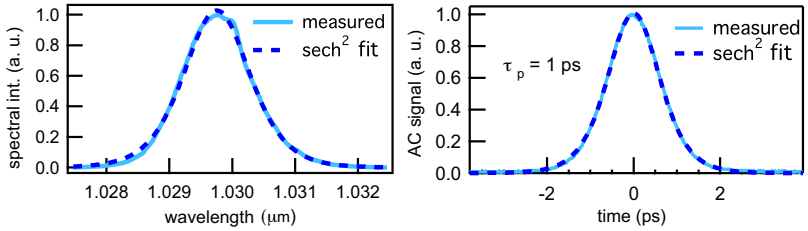

Fig. 1. Seed Laser. Right: Autocorrelation trace of the seed pulses. Left: Corresponding spectrum.

The average power obtained from this seed laser is sufficient to directly saturate the amplifiers used in both setups without the need for pre-amplifier stages. The complexity of such an oscillator is comparable to that of a low-power oscillator. Therefore, the resulting compression and amplification setup is relatively simple with high average powers at a low overall amplifier gain, which is beneficial for low parasitic nonlinear effects and for a clean spectral broadening. Despite the fact that the laser was built with standard opto-mechanical components on a laboratory breadboard, it did not require any realignment during the several weeks of operation.

2.1 First amplifier system: 2200 µm^2 core area rod-type fiber delivering 55 W, 98 fs, 5.2 µJ, 10.6 MHz, 32.7 MW peak power)

The high-power thin disk laser was used to seed a 55-cm long polarization maintaining Yb-doped rod-type LMA fiber amplifier in a counter-propagating configuration (Fig. 2). The rod was cleaved at 5 degrees at the input end to avoid parasitic lasing and had an uncleaved 8-mm-long end-cap on the output side. The signal core had a diameter of 70 µm and a pump cladding diameter of 200 µm. In order to avoid damage of the rod and self-focusing the input

#138059 - $15.00 USD Received 15 Nov 2010; revised 16 Dec 2010; accepted 20 Dec 2010; published 12 Jan 2011

pulses were stretched to 1.9 ps FWHM using two 1250 l/mm transmission gratings in a negative dispersion configuration [31].

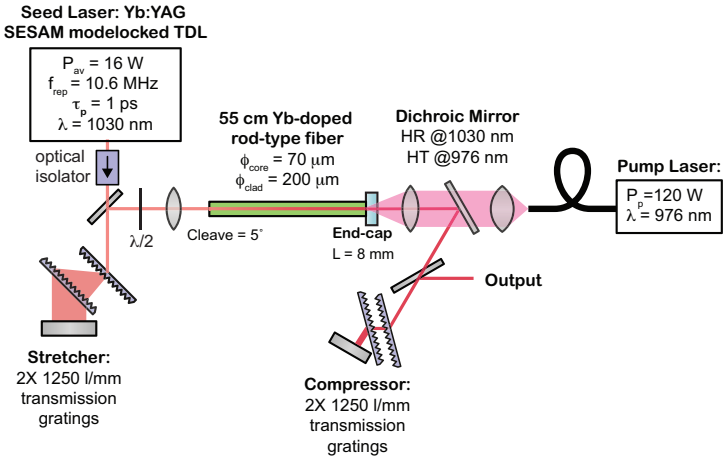

Fig. 2. First compressor amplifier system, based on the 55-cm long rod-type fiber.

In standard CPA systems, positive chirp is usually preferred for stretching the input pulses. In this case, SPM broadening occurs over the entire length of the fiber, and the amount of accumulated SPM is easy to control since it is nearly linear. Negatively chirped pulses lead to an initial spectral and temporal narrowing before the linear SPM broadening starts to occur. In Fig. 3, we simulated the effect on the spectral FWHM bandwidth over the length of the fiber for negatively or positively chirped input pulses, using a home-made split-step Fourier propagation software. In the case of negatively chirped pulses the spectrum undergoes a minimum after a few centimeters of propagation through the fiber (Fig. 3 bottom left, inset). The spectral narrowing that occurs in the first 15 cm of the rod is negligible.

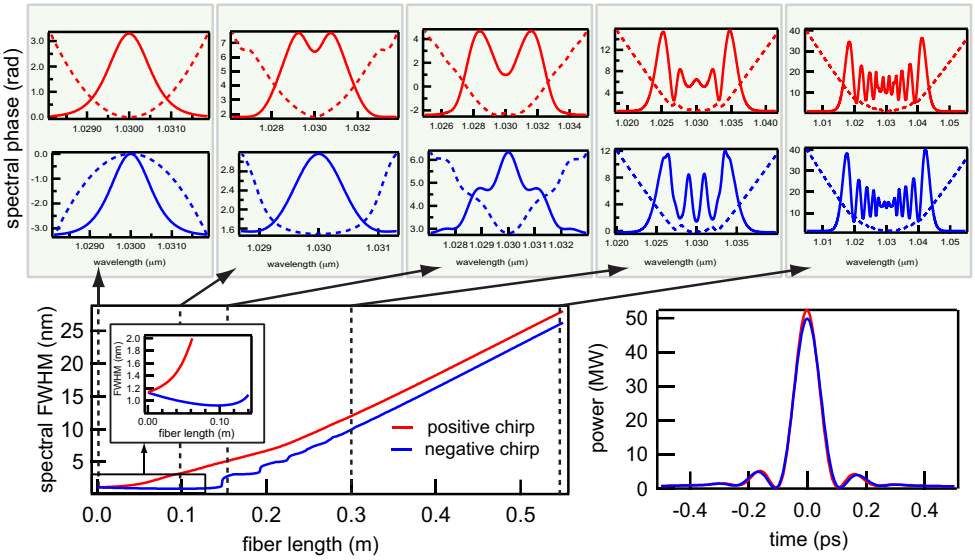

Fig. 3. Simulation of the effect of the input sign of the chirp on the spectral broadening in the rod-type fiber amplifier. Bottom (left): Evolution of the spectral FWHM during propagation in the rod for negatively (blue) and positively (red) chirped pulses. Top (left to right): Evolution of the spectral intensity and the spectral phase during propagation in the fiber for positively and negatively chirped pulses. Bottom (right): resulting compressed power after 55 cm of propagation for negatively and positively chirped pulses. These simulations were performed with our home-programmed split-step Fourier propagation software.

#138059 - $15.00 USD Received 15 Nov 2010; revised 16 Dec 2010; accepted 20 Dec 2010; published 12 Jan 2011

In this experiment, we chose to use negatively chirped pulses to simplify the grating stretcher since the two configurations result in similar compression factors, as can be seen in Fig. 3 where the resulting compressed pulses are shown (bottom, right). The total transmission through the stretcher was measured to be 75% reducing the power launched into the fiber to 12 W.

The pump used for the amplification delivers 120 W at 976 nm. The performance of the fiber amplifier is shown in Fig. 4. We achieved 73 W of average output power, which corresponds to a pulse energy of 6.85 μJ. The output of the fiber amplifier was polarized, and we measured a Polarization Extinction Ratio (PER) of 15.8 dB. At this power level an optical-to-optical efficiency $\eta_{opt} = \frac{P_{out}}{P_{pump} + P_{seed}}$ of 56.6% is reached with a slope efficiency of 61%. The pulses after amplification are slightly stretched to 2.7 ps due to dispersion in the rod. At the output of the rod the peak power is 2.2 MW, corresponding in the 2200 μm^2 core to an intensity of approximately 2 $kW/\mu m^2$. At this peak power, no signs of self-focusing are observed and the beam quality stayed close to the diffraction limit with a measured $M^2 = 1.3$.

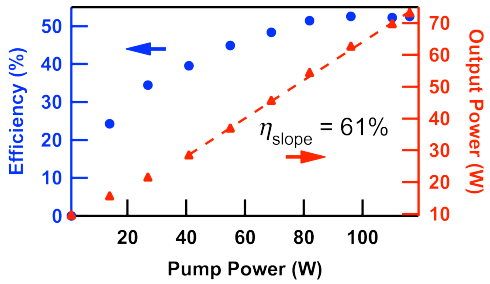

Fig. 4. Measured output power slope of the fiber amplifier. The maximum output power of 73 W corresponds to an optical-to-optical efficiency of 56.6%.

The double pass compression stage consists of two 1250 l/mm transmission gratings as used for the input stretcher [31]. The transmission gratings are 100% fused silica and have low absorption, which is beneficial at the high power levels considered. The use of 1250 l/mm gratings enables a very compact compressor setup. The necessary dispersion was obtained with a grating distance of 3.2 mm. In a standard SF10 prism compressor several meters between the prisms would be necessary to obtain enough negative dispersion. The total transmission through the 4-pass compressor was measured to be 75.4%. The resulting output power after compression was 55 W, corresponding to a pulse energy of 5.2 μJ. The obtained pulses after compression were characterized using an SHG FROG [32] and the obtained results are presented in Fig. 5. The retrieved FROG trace shows a FWHM pulse duration of 98-fs and a peak power of 32.7 MW (taking into account the energy distribution of the exact pulse shape as shown in Fig. 5). The retrieved pulses are compared to the Fourier limit of the measured spectra after the amplifier and to simulations performed using a home-programmed split-step Fourier nonlinear propagation software. The values used for coupling efficiencies were typical values of η_{pump} = 70% and η_{seed} = 80%. The simulated compression is done using negative second order dispersion and optimizing for peak power. A comparison of the different parameters obtained is presented in Table 1.

#138059 - $15.00 USD Received 15 Nov 2010; revised 16 Dec 2010; accepted 20 Dec 2010; published 12 Jan 2011

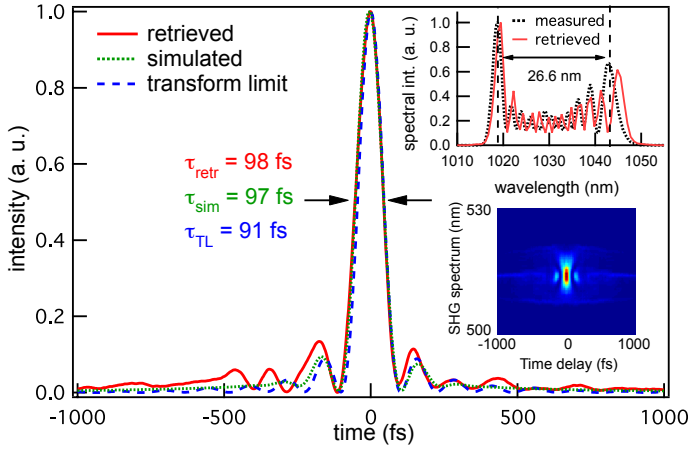

Fig. 5. SHG FROG characterization of the compressed pulses at the maximum output power of 55 W. Bottom right inset: Measured FROG trace. The FROG grid used was 256x256, and the retrieved error was 7.10^{-3}. Top right inset: measured spectrum at maximum output power.

Table 1. Different pulse characteristics of the retrieved, simulated and transform-limited pulses for the 55-cm rod-type amplifier

	Retrieved	Transform-limit	Simulated
Pulse FWHM	98 fs	91 fs	97 fs
Peak Power	32.7 MW	43.2 MW	37.9 MW
Energy in the main pulse	66%	81%	77%
Strehl ratio	0.76	-	0.87

As can be seen in Fig. 5 and Table 1, a residual picosecond background in the pulse limits the amount of energy in the main pulse to only 66%. This leads to a temporal Strehl ratio (corresponding to the ratio between the peak power obtained and the peak power of the transform-limited pulse corresponding to the measured spectrum [33]) of 0.76. According to the simulations a Strehl ratio of 0.87 could be achieved with the measured spectrum considering only second-order dispersion. The difference to the transform-limit is partly due to the uncompensated third-order dispersion. We can see in the top-right inset of Fig. 9 below that the retrieved spectrum and the independently measured spectrum using an optical spectrum analyzer are in good agreement. The system was operated for around one hour before damage was observed. This made precise optimization of the gratings difficult at this power level. Nevertheless, the pulses obtained are in good agreement with the performed simulations and peak powers >30 MW were obtained in this way. On the other hand, although higher peak powers seem to be feasible with this system, two rods were damaged at this output power level, indicating that the system is operating close to its damage limit, and is not suitable for further amplification and/or compression to shorter pulses. More details on the observed damage behavior will be discussed in a next paragraph.

2.2 Second stretcher-free amplifier system: 4500 μm^2 core area rod-type fiber delivering 34 W, 65 fs, 3.2 μJ, 10.6 MHz, 32 MW peak power

The second fiber amplifier system consisted of a shorter (36 cm) polarization maintaining rod-type fiber with a larger core diameter of 100 μm and a resulting mode field area A = 4500 μm^2 which is two times larger than in the previous setup. The pump cladding is also larger with a diameter of 285 μm. The rod has two uncleaved 8-mm end-caps at the input and output facets.

#138059 - $15.00 USD Received 15 Nov 2010; revised 16 Dec 2010; accepted 20 Dec 2010; published 12 Jan 2011

Although the input end-cap is beneficial to prevent damage of the rod due to the seed laser pulses, the peak power levels at the input of the rod should not reach critical damage levels. At the output facet, the presence of an end-cap is crucial to avoid damage of the rod. Furthermore, the larger core size should limit the probability for bulk and surface damage of the rod by operating at lower intensities for a given peak power. Furthermore, the larger core size combined with a shorter fiber length allows for enough spectral broadening to generate sub-100 fs pulses in a simpler setup where no stretching of the seed laser pulses is necessary. The setup is shown in Fig. 6.

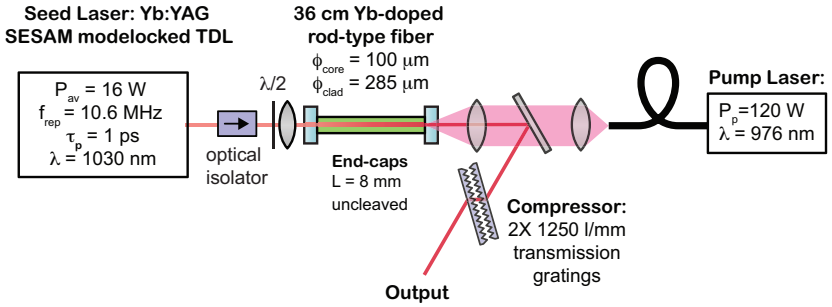

Fig. 6. Second compressor amplifier system: the 36-cm fiber amplifier with a core area of 4500 μm^2 is seeded directly with the high-power thin disk laser oscillator. The compressor stage consists of a single pass through two transmission gratings.

We launched the full seed laser power into the fiber (15 W of launched power). The performance of the fiber amplifier is shown in Fig. 7. The full power of the pump was not used in order to avoid damage of the rod and/or self-focusing effects. We therefore limited the launched pump power to an amplification leading to an output power of approximately 40 W, corresponding to 3 MW of peak power at the end of the rod. This value is to be compared to the reported approximate critical self-focusing peak power of 4 MW [34].

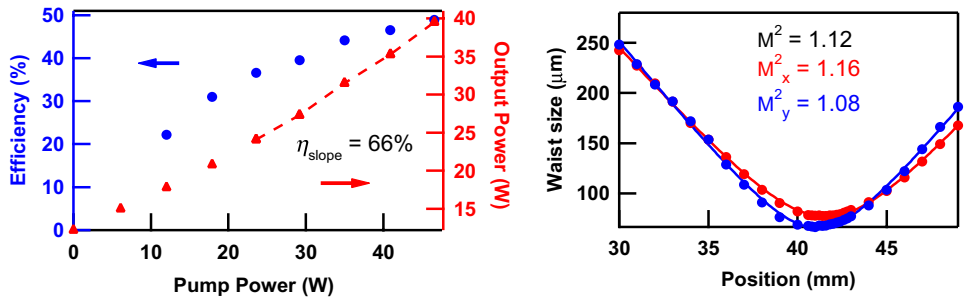

Fig. 7. Left: Fiber amplifier performance Right: M^2 measurement of the output of the fiber at the maximum output power level of 39.5 W.

In spite of the shorter fiber length, good amplification performance could be obtained from this system. At an output power of 39.5 W, the optical-to-optical efficiency reaches 48.8% (Fig. 7 left). The output of the fiber amplifier was close to the diffraction-limit with a measured M^2 <1.2 at the maximum output power level (Fig. 7 right) and was linearly polarized with a measured PER of 10 dB. The slight degradation of the PER observed at these high peak powers compared to the previous system is probably due to remaining mechanical stress from the fiber mount on the rod, which can degrade the polarization maintaining feature for the extremely large core areas considered. Although the amplifier is not totally saturated at this power level, we limited ourselves to this output power to avoid damage of the rod. The 1-ps input pulses are slightly stretched to 1.5 ps at the maximum power level due to dispersion in the fiber. The spectral broadening that occurs with amplification is shown in Fig. 8. Without any amplification, propagation of the seed pulses already generates more than 20 nm of spectrum due to SPM. At the maximum output power we observed over 35 nm of spectral

#138059 - $15.00 USD Received 15 Nov 2010; revised 16 Dec 2010; accepted 20 Dec 2010; published 12 Jan 2011

broadening and some spectral shaping due to the gain spectrum of the fiber, which makes the spectrum asymmetric at higher output powers.

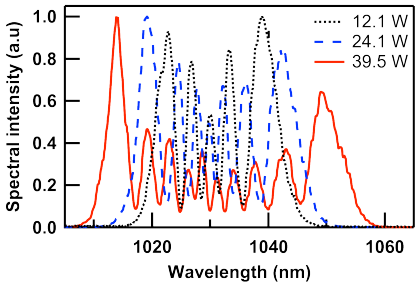

Fig. 8. Observed spectral broadening at different output powers. We also observe some spectral shaping probably due to the gain bandwidth.

The compression stage consists of a single pass two-grating compressor [31]. The gratings used are 1250 l/mm transmission gratings. In order to compress the pulses at the maximum output power, the negative dispersion needed is approximately $-16'000$ fs^2, which corresponds to a grating distance of approximately 1.3 mm in a double-pass configuration. At the expense of some spatial chirp that can be neglected, the compression scheme used was a one-pass two-grating compressor with a distance between the gratings of 2.6 mm. In this case, the measured spectrum at full power extends spatially over 170 µm. This can be neglected over a total beam diameter of 1.9 mm. With this compression scheme we achieved a compression efficiency of 86% at full power, and a resulting compressed power of 34 W. The compressed pulses were characterized using an SHG FROG [32]. The retrieved pulses can be seen in Fig. 9 and are compared to the transform-limited pulse of the measured spectrum and the simulated pulses using the same software described for the first setup. The different pulse parameters are summarized in Table 2.

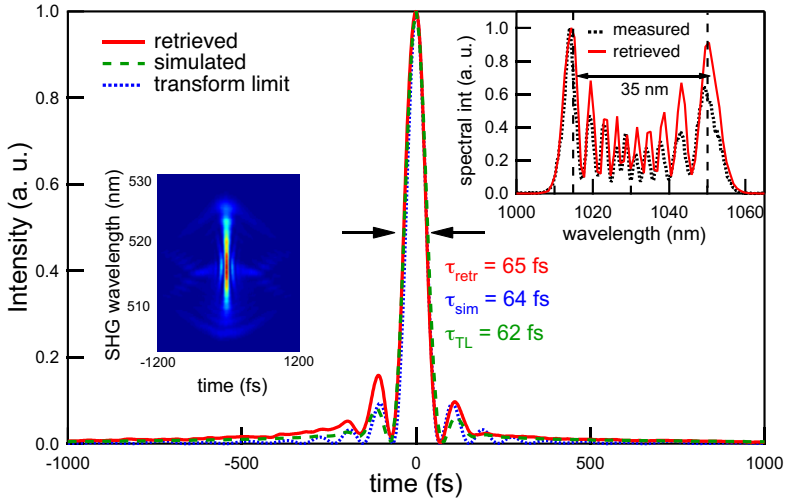

Fig. 9. SHG FROG characterization of the compressed pulses at the maximum compressed power of 34 W. Bottom right inset: Measured FROG trace. The FROG grid used was 256x256, and the retrieved error was 4.10^{-3}. Top right inset: measured spectrum at maximum output power.

#138059 - $15.00 USD Received 15 Nov 2010; revised 16 Dec 2010; accepted 20 Dec 2010; published 12 Jan 2011

Table 2. Different pulse characteristics of the retrieved, simulated and transform-limited pulses for the 36-cm rod-type stretcher-free amplifier system

	Retrieved	Transform-limit	Simulated
Pulse FWHM	65 fs	62.8 fs	60.5 fs
Peak Power	32 MW	39.3 MW	37.5 MW
Energy in the main pulse	65%	79%	72%
Strehl ratio	0.81	-	0.91

The retrieved pulses have a FWHM duration of 65 fs, with 65% of the total amount of energy within the main pulse resulting in 32 MW of peak power. Although this value is lower than for the previous setup, the resulting Strehl-ratio of 81% shows that we are closer to the transform-limited case. A better Strehl ratio could be obtained by carefully optimizing third-order dispersion of the system, especially for these shorter pulse durations. We can see in the top-right inset of Fig. 9 that the retrieved spectrum and the independently measured spectrum using an optical spectrum analyzer are in good agreement. The residual spatial chirp of the compressed beam can probably account for the small difference observed in the peak heights. Nevertheless, the accumulated nonlinear phase is confirmed. The pulses obtained show a good agreement with pulse propagation simulations carried out with the same software as described for the first setup. The small difference observed can probably be accounted for by the spectral asymmetry observed in the measured spectrum that is not present in the simulations, since the software does not take into account the gain bandwidth.

3. Further scaling of these systems: damage and self-focusing considerations

The main energy limitations of the systems described in this paper are due to operation of these fiber amplifiers at very high peak powers, close to the intrinsic damage thresholds and critical self-focusing. Many investigations on fiber damage have been carried out in order to establish guidelines on how to avoid these detrimental effects [34,35]. However, threshold values are always strongly dependent on experimental conditions such as pulse parameters, coupling conditions, and doping concentration, which is of particular importance to fiber amplifiers. We have summarized the different relevant operation parameters of these two fiber amplifier systems in Table 3, which identify the different mechanisms that currently limit further power scaling.

Table 3. Operation points at maximum output power and reported damage parameters

	2200 μm^2 core rod	4500 μm^2 core rod	Critical threshold
Peak power (output of the rod)	~2.2 MW	~3 MW	~4 MW [34]
Peak intensity (before end-cap)	~2 kW/μm^2 (= $2 \cdot 10^{11}$ W/cm^2)	~1.2 kW/μm^2 (= $1.2 \cdot 10^{11}$ W/cm^2)	> 2 kW/μm^2 [36] (= $2 \cdot 10^{11}$ W/cm^2)
Peak intensity (after end-cap)	~40 W/μm^2 (= $4 \cdot 10^{9}$ W/cm^2)	~44 W/μm^2 (= $4.4 \cdot 10^{9}$ W/cm^2)	
Observations	Damage	No Damage	

There are mainly three possible reasons for damage or beam degradation in fiber systems operated at high peak power levels: self-focusing, surface or bulk damage. Concerning self-focusing, the critical peak power threshold commonly used for silica fibers is 4 MW [34,35] The manufacturer reported values in the order of several hundred W/μm^2 for the surface damage threshold peak intensity of similar Yb-doped cores without an end-cap [36].

#138059 - $15.00 USD Received 15 Nov 2010; revised 16 Dec 2010; accepted 20 Dec 2010; published 12 Jan 2011

In the case of the 55-cm rod with a core area of 2200 μm^2, damage was observed at the same intensity level in two different occasions. In both cases, the damaged area was inside the rods and close to the interface between the end-cap and the rod where the maximum intensity reaches 2 kW/μm^2 The peak power of 2.2 MW does not reach values where significant beam degradation due to self-focusing is observed, which seems to indicate that the bulk damage threshold has been reached.

In the case of the 36-cm rod with a core area of 4500 μm^2, neither damage nor beam degradation was observed at an even higher peak power of 3 MW. At this level, self-focusing does not seem to affect the beam quality at the output of the amplifier. The corresponding maximum intensity is 1.2 kW/μm^2, which is 60% lower than the value where damage was observed for the previous fiber. However, if we consider further power scaling of this system, beam degradation due to self-focusing might be apparent before surface or bulk damage are reached [34].

In the stretcher-free configuration with the input pulse parameters of our thin disk laser, an increase in average output power would potentially result in damage or self-focusing. Therefore, the only possible approach to scale the compressed peak power is to increase the spectral broadening at this fixed maximum output power level.

In the system presented here, we clearly benefit from the high initial output energy of the oscillator that saturates the amplifier and enables important spectral broadening. Fig. 10 (left) clearly shows the benefit in peak power with higher seed power for constant average output power and constant rod length. The output power is kept constant by adapting the pump power. A higher input power corresponds to a lower overall gain. As we can see in the simulations, the peak power is increased for a higher input power.

In our system we could also increase the peak power by increasing the length of the rod. In Fig. 10 (right) we simulated the effect of increasing the length of the rod at a given pump and input power. As we can see, an increase of a factor of two in fiber length (from 300 mm to 600 mm) results in an output power increase of approximately 10%. We experience a higher benefit for the compressed peak power by more than a factor of two, because of the additional SPM accumulated in the longer rod. However, only a 36-cm-long rod was available at the moment, and one should also consider that using a too long rod might lead to parasitic nonlinear effects such as Raman scattering.

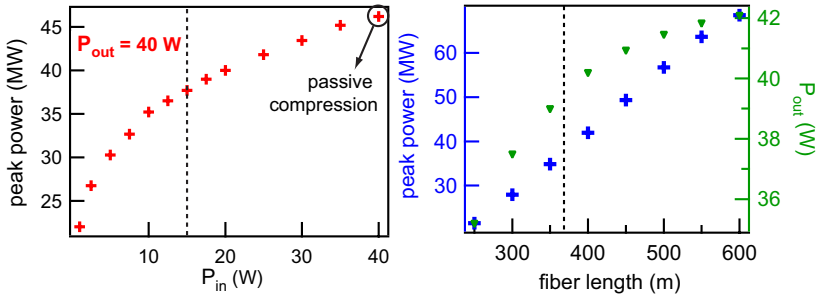

Fig. 10. Simulations performed with the home-programmed split-step Fourier software described in paragraph 2. Left: compressed peak power as a function of the input average power for a given average output power. Right: compressed peak power and average output power as a function of the fiber length.

4. Conclusion and Outlook

We have presented two systems for pulse compression of a thin disk oscillator and discussed the performance as well as the main limitations of these systems. The results are summarized in Table 4.

#138059 - $15.00 USD Received 15 Nov 2010; revised 16 Dec 2010; accepted 20 Dec 2010; published 12 Jan 2011

Table 4. Summary of the results obtained with the two rod-type fiber amplifier systems

	System 1	System 2
Length of fiber amplifier	55 cm	36 cm
Core diameter	70 μm	100 μm
Input average power (launched)	12 W	15 W
Input pulse duration	1.9 ps	1 ps
Maximum output average power	73 W	39.5 W
Output pulse duration	2.7 ps	1.5 ps
Output peak power	2.2 MW	3 MW
Compressed average power	55 W	34 W
Compressed pulse duration	98 fs	65 fs
Compressed energy	5.2 μJ	3.2 μJ
Compressed peak power	32.7 MW	32 MW
Strehl ratio	0.76	0.81
Limitation	Damage	-

The seed laser used in both cases consists of a standard Yb:YAG thin disk laser and delivers 16 W of average power at a pulse repetition rate of 10.6 MHz and a laser wavelength of 1030 nm. The resulting pulse energy is 1.6 μJ in 1-ps long pulses.

The first compression system consists of a 55-cm-long polarization-maintaining rod-type fiber amplifier with a core size diameter of 70 μm. We used the minimum stretching factor of the input pulses to avoid damage of the rod. We obtained, in this case, 55 W of compressed average power in 98-fs pulses, corresponding to a peak power of 32.7 MW and a pulse energy of 5.2 μJ. The main limitation of this system was damage observed at the highest average output power indicating operation close to the bulk damage threshold of silica.

In the second compression setup, we used a shorter rod-type fiber (36 cm) with a larger core size diameter of 100 μm, leading to a core area 2 times larger than for the 55-cm rod. This allowed us to directly seed the amplifier without stretching the input pulses. With this setup we achieved 34 W of compressed average power and pulses with a duration 65-fs pulses leading to 32 MW of peak power. The larger core size allowed for a simpler stretcher-free configuration, where damage could be avoided at similar peak power levels in the rod. Nevertheless, self-focusing may be apparent in this case before damage can occur, which is one of the reasons why we limited the output average power to 40 W before compression. Stretching the input pulses to generate a lower peak power at the output facet of the fiber would represent an alternative to safely increase the output average power. However, this would be at the expense of simplicity of the setup.

In both amplifiers a compromise in peak power in the rod had to be made. In order to reach a high compression factor, significant peak power in the fiber is needed. The maximum applicable peak power is set by damage and/or self-focusing. Furthermore, the goal was to achieve high pulse energies (typically > 3 μJ) after compression in the simplest possible configuration. Therefore the stretcher-free approach was preferred. Given these design parameters, the performance obtained from each system were specific to each experiment and to the corresponding risks that were taken. In both systems, we could achieve peak power levels >30 MW at several μJ pulse energy. The high-power SESAM modelocked thin disk laser used as a seed for both amplifiers allowed for simple setups where the oscillator directly saturates the main amplifier and generates enough spectral broadening to support sub-100 fs pulses.

One could think of operating such an amplifier system in the parabolic regime where the obtained chirp due to the spectral broadening is quasi-linear and the quality of the compressed pulses is higher. However, for the picosecond source and $sech^2$-shaped seed pulses this would

#138059 - $15.00 USD Received 15 Nov 2010; revised 16 Dec 2010; accepted 20 Dec 2010; published 12 Jan 2011

require the use of long fibers, and parasitic nonlinear effects such as Stimulated Raman scattering (SRS) might degrade the convergence to the parabolic regime [37]. In this case, the use of a thin disk seed laser with shorter pulses would be beneficial. Furthermore, the gain bandwidth limitation makes the compression schemes in this regime more challenging [26,38].

Another approach would be to extend the work on passive LMA fiber compression, by using passive large mode area rods directly seeded by higher energy seeds, such as for instance the demonstrated oscillator delivering 10 μJ pulse energy [12]. The high peak power levels of this system would require stretched pulses of approximately 3 ps in order to avoid self-focusing. This larger stretching ratio makes a good compression quality to sub-100-fs challenging. Using a passive rod with 4500 μm^2, our simulations predict that after 80 cm of propagation we would obtain 85 fs pulses with 80 MW peak power. However, the passive rod-fiber development has not received the same attention as the fiber amplifiers, which limits their availability.

Although high peak powers were obtained with this setup, the limitations of these systems seem to indicate that further peak power scaling to sub-50 fs pulses and/or higher energies require other compression schemes such as compression in gas-filled hollow core fibers [39] filament compressors [40] or OPCPA techniques [11].

Acknowledgments

We would like to acknowledge financial support by the Swiss National Science Foundation (SNF) and thank Dr. Kim P. Hansen and Dr. Arlee V. Smith for helpful discussions on fiber damage.

#138059 - $15.00 USD Received 15 Nov 2010; revised 16 Dec 2010; accepted 20 Dec 2010; published 12 Jan 2011